Front bifurcation in a tristable reaction-diffusion system under periodic forcing

E. P. Zemskov*

Institut für Theoretische Physik, Otto-von-Guericke-Universität, Universitätsplatz 2, 39106 Magdeburg, Germany

(Received 11 August 2003; published 30 March 2004)

A piecewise linear tristable reaction-diffusion equation under external forcing of periodic type is considered. A special feature of the forcing is that the force moves together with the traveling wave. Front velocity equations are obtained analytically using matching procedures for the front solutions. It is noted that there is a restriction in building of null-cline. For each choice of outer branches of null-cline the middle interfacial zone should not exceed some critical value. When this zone is larger the front does not exist. It is found that in the presence of forcing there exists a set of front solutions with different phases (matching point coordinates). The periodic forcing produces a change in the velocity-versus-phase diagram. For a specific choice of wave number, there is a bubble formation which corresponds to additional solutions when the velocity bifurcates to form three fronts.

DOI: 10.1103/PhysRevE.69.036208 PACS number(s): 05.45.−a, 47.20.Ma, 47.54.+r

I. INTRODUCTION

Reaction-diffusion equations belong to a family of single-component models of broad applicability. Single-species models are of relevance to laboratory studies in particular but, in the real world, can reflect a telescoping of effects which influence the reaction kinetics [1]. Fronts, the elementary structures described by reaction-diffusion equations, are known in diverse systems [2,3]. There are two basic types of fronts: the front propagating into a stable state and into an unstable state. In the first case the front has a unique velocity and in the second case there is a continuum of possible velocities [2]. The example of front propagation into an unstable state exhibits the Fisher equation with quadratic nonlinear reaction term. The equation describing the front propagation into a stable state has cubic nonlinearity and named as a bistable model. Our interest in the present paper is in a generalization of the bistable model to a multistable case. Traveling fronts in one-variable multistable reaction-diffusion system were investigated numerically by Leda and Kawczyński [4]. Besides solutions of the model equation being single traveling fronts, their possible compositions with different velocities were considered. Such compositions can give monotonic or nonmonotonic solutions. We restrict here our consideration to the situation with equal velocities and will consider here a simplest case of the multistable model—a tristable equation, which possesses three locally stable states with two unstable states. A realistic chemical model of the tristable system consists of two enzymatic reactions inhibited by an excess of their reactant [4]. Two different enzymes catalyze transformations of a reactant into two different products according to the Michaelis-Menten kinetics. Both active complexes are inhibited by an excess of the reactant. The detailed chemical reaction scheme is presented in Ref. [4].

A global view of the nature and multiplicity of front solutions in the one-component reaction-diffusion model can be obtained with a well-known simple particle-in-a-potential analogy [2]. This analogy is based on the identification of traveling wave equation with the equation of motion of a classical particle with friction in a potential. For the bistable system we have a potential of the double-hill shape (a potential with two maxima) and in the case of tristable model—a triple-hill potential. The triple-well potential was considered in Ref. [5] to compute quantum-mechanical problems using instanton solution. In Ref. [6] the nonlinear Klein-Gordon equation describing a massive real scalar field with u^4-u^6 self-coupling was examined and first-order phase transitions were studied. In our paper we report on a solution of a different type of problem, namely the reaction-diffusion equation.

Wave propagation in the reaction-diffusion systems can be effectively controlled by application of an external forcing [7–10]. This forcing can be prescribed *a priori* (i.e., as a periodic modulation of excitability [8,9]) or computed online using the data of the momentary state of the medium by closing a feedback loop [10,11]. The phenomenology of this situation is well known. The properties of an external forcing can be studied experimentally by using the light-sensitive Belousov-Zhabotinsky reaction for which the absorption of transmitted light depends on the concentration of chemical species [11].

Having in mind that a general irregular forcing may be represented via Fourier decomposition as a superposition of harmonically oscillating ''modes,'' it is instructive to investigate the wave behavior under a periodically oscillating forcing. The case of a force oscillating with time was examined in Refs. [8,9,12]. A ''pulling effect'' [12] of the fronts was found: it was shown that the mean velocity of the perturbed front is increased as compared to that of the unperturbed front. Effectively, the case of time-dependent forcing describes a time-dependent excitability, i.e., a null-cline (equal to zero reaction term) with periodically oscillating constants. In our paper, we study another interesting case of periodic forcing, namely one that is nonmoving in the comoving frame, i.e., moving together with the traveling wave. This type of the forcing is given the name ''comoving forcing.'' The comoving forcing imagination is as follows. Starting from the stationary wave solution the velocity is used as

*Email address: zemskov@physik.uni-magdeburg.de

a control feedback parameter for the deviation of a spatially extended light source from its position at the position at the stationary case, so that the light source moves together with the wave in the excitable medium. The comoving forcing differs in significant ways from parameter-dependent (time or spatial) forcings. The problem becomes an inhomogeneous one and the general solution of the traveling wave equation acquires an additive part. When the wave speed is equal to zero the system degenerates into the spatially forced one. In this case the external forcing can be regarded as a spatial inhomogeneity which brings the traveling fronts to a stop (front pinning).

Our approach will be analytical rather than numerical. This is possible since the nonlinear reaction term is a piecewise linear function. Piecewise linear dynamics may be used for a variety of nonlinear systems, and have been employed in a number of situations [13–18]. Although piecewise linear systems are at best caricatures of the desired model dynamics, there is the strong advantage that one can reduce existence problems for traveling waves to root finding for certain nonlinear algebraic equations. Before the present study, no full analytic solutions of the periodically forced tristable equation were available. In our paper we do not address the general initial value problem. Instead, our interest is in finding the traveling wave solutions and explorations into the influence of the external periodic forcing. The stability analysis of the tristable fronts was also performed and will be reported elsewhere.

II. BASIC FRONT SOLUTIONS

We consider one-component one-dimensional medium, which is described by reaction-diffusion equation of parabolic type. At first, we shall consider the tristable medium to be homogeneous, i.e., without forcing. A diffusion coefficient is constant and we set it equal to unity. Thus, our system consists of one scalar field $u=u(x,t)$ and is described by the equation

$$\frac{\partial u(x,t)}{\partial t}=f(u)+\frac{\partial^2 u(x,t)}{\partial x^2}, \tag{1}$$

where the reaction term $f(u)$ is a piecewise linear function $f(u)=-u-b_1+b_1\theta(u+u_{1-2})+b_3\theta(u-u_{2-3})$ and b_1,b_3,u_{1-2},u_{2-3} are constants. The null-cline $f(u)=0$ is shown in Fig. 1(a). Here $\theta(u)$ is the Heaviside step function, i.e.,

$$f(u)=\begin{cases}-u-b_1, & u<-u_{1-2}\\ -u, & -u_{1-2}<u<u_{2-3},\\ -u+b_3, & u>u_{2-3}.\end{cases}$$

Due to a piecewise linear character of the reaction term $f(u)$ we can easily obtain the solution for each piece. We introduce the traveling frame coordinate $\xi=x-ct$, where c is the front velocity, and rewrite Eq. (1) for the propagating solution $u(\xi)$ as

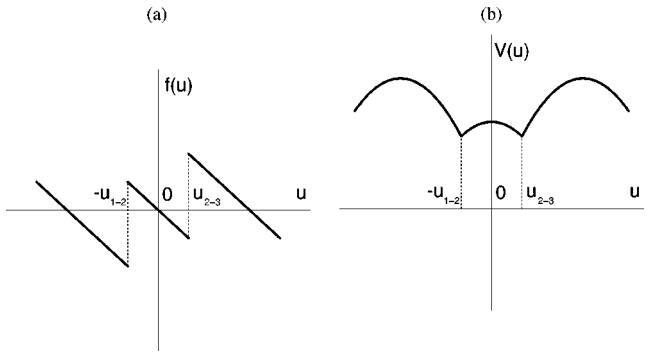

FIG. 1. Tristable model: (a) piecewise linear null cline $f(u)=0$ and (b) corresponding matched piecewise parabolic potential $V(u)$. Symmetric case, $b_1=b_3$ and $u_{1-2}=u_{2-3}$.

$$\frac{d^2u(\xi)}{d\xi^2}+c\frac{du(\xi)}{d\xi}+f(u)=0. \tag{2}$$

There exist different front solutions of the tristable equation. First of all, there is a front propagation between $u=-b_1$ and $u=0$. This front is described by the bistable model and we do not consider it here. The second case is just an extension of the bistable front to the tristable model. This front solution interpolates from $u=-b_1$ as $\xi\to-\infty$ to $u=b_3$ as $\xi\to+\infty$ and consists of three pieces. We shall name it the 3-front (monotone front). The distinguishing feature of the tristable model is the possibility of the front between $u=-b_1$ and $u=0$ passing through all three zones. This front consists of four pieces and we name it the 4-front (nonmonotone front). First we consider the 3-front. The solution reads

$$u_1(\xi)=A_1e^{\lambda^+\xi}-b_1, \quad \xi\leqslant\xi_0,$$

$$u_2(\xi)=A_{21}e^{\lambda^+\xi}+A_{22}e^{\lambda^-\xi}, \quad \xi_0\leqslant\xi\leqslant\xi_0^*, \tag{3}$$

$$u_3(\xi)=A_3e^{\lambda^-\xi}+b_3, \quad \xi\geqslant\xi_0^*,$$

where $\lambda^{\pm}=-c/2\pm\sqrt{c^2/4+1}\equiv-c/2\pm\gamma$. To construct the front solutions from three pieces we impose the matching conditions for the functions $u_i(\xi), i=1,2,3$ and their derivatives $du_i(\xi)/d\xi$ at points $\xi=\xi_0$ and $\xi=\xi_0^*$, where the two neighbor parts of the solution are patched together:

$$u_1(\xi_0)=u_2(\xi_0), \quad u_2(\xi_0^*)=u_3(\xi_0^*),$$

$$\frac{du_1(\xi_0)}{d\xi}=\frac{du_2(\xi_0)}{d\xi}, \quad \frac{du_2(\xi_0^*)}{d\xi}=\frac{du_3(\xi_0^*)}{d\xi}, \tag{4}$$

i.e., we require continuity of the solution and its derivative. Two additional equations are obtained using the fact (as was done in previous works, see Refs. [17]) that we know the $u(\xi)$ values of the matching points:

$$u_1(\xi_0)=-u_{1-2}, \quad u_3(\xi_0^*)=u_{2-3}. \tag{5}$$

Due to translational invariance of the basic equations, the position of one matching point can be chosen arbitrarily, and we choose $\xi_0=0$. This is a consequence of the homogeneity of the model.

From the matching conditions the unknowns A, c, and ξ_0^* may be determined and explicitly expressed as functions of the null-cline parameters b_1, b_3, u_{1-2}, u_{2-3}. Reducing the number of equations from six to one, we obtain a relationship for the front velocity c (see the Appendix),

$$\lambda^- \ln\left[\frac{b_3\left(1+\frac{c}{2\gamma}\right)}{2A_{21}}\right]=\lambda^+\ln\left[\frac{b_3\left(1-\frac{c}{2\gamma}\right)}{2(A_{22}-A_3)}\right], \qquad (6)$$

where constants A are functions of c and derived in the Appendix.

During derivation of Eq. (6), it was noted that $(1+c/2\gamma)/A_{21}$ and $(1-c/2\gamma)/(A_{22}-A_3)$ must be positive magnitudes. This condition restricts the choice of the null-cline. So, in the case of stationary front ($c=0$) this restriction condition gives us $u_{1-2}<b_1/2$ and $u_{2-3}<b_3/2$, i.e., for each choice of the outer branches of the null-cline the middle interfacial zone of the front should not exceed some critical value $u_{\rm crit}$. When the size of the middle interfacial zone $u_{1-2}+u_{2-3}\equiv u_0$ is larger than this critical value the front does not exist. A view of the origin of the restriction condition can be obtained with a particle-in-a-potential analogy. The reaction term $-f(u)$ represents a force in this analogy. The potential $V(u)=\int f(u)du$ is piecewise parabolic type,

$$V(u)=\begin{cases} -u^2/2-b_1u+h_1\equiv V_1(u), & u<-u_{1-2} \\ -u^2/2+h_2\equiv V_2(u), & -u_{1-2}<u<u_{2-3} \\ -u^2/2+b_3u+h_3\equiv V_3(u), & u>u_{2-3}, \end{cases}$$

where h_i, $i=1, 2, 3$, are arbitrary constants. For the sake of simplicity we consider here the symmetric case. In this situation $h_1=h_3$ and we choose $h_1=h_3=0$. The constant h_2 may be determined using the matching condition for the potential $V(u)$: $V_2(u_{2-3})=V_3(u_{2-3})$. From this equation we obtain $h_2=b_3u_{2-3}$. The same condition takes place for another matching point at $u=u_{1-2}$. The obtained potential is shown in Fig. 1(b). The maxima of V_2 and V_3 lay at 0 and b_3, respectively. When the maximum of the outer branch is higher than the maximum of the middle zone we obtain $V_3(b_3)-V_2(0)=b_3^2/2-b_3u_{2-3}>0$. Hence the above-stated restriction condition $u_{2-3}<b_3/2$ follows. Thus, the front between two outer branches may exist *only* when the middle maximum of the potential is a *local* one.[1]

Front solution (3) is presented graphically in Fig. 2. As earlier in the case of the bistable model when the null cline is symmetric (i.e., when $u_{1-2}=u_{2-3}$ and $b_1=b_3$) the front is stationary ($c=0$), namely this case is shown in Fig. 2, and when the null-cline is asymmetric (as example, when u_{1-2}

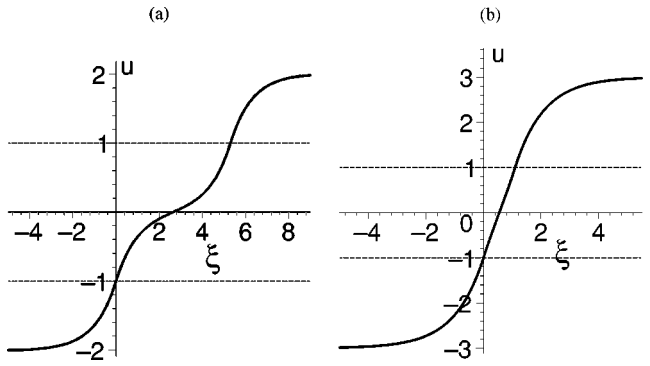

FIG. 2. Front solution (3) when the middle interfacial zone (a) $u_0\simeq u_{\rm crit}$ and (b) $u_0\ll u_{\rm crit}$ in the case of symmetric null-cline (motionless fronts). The dashed lines represent the boundary values $u=-u_{1-2}$ and $u=u_{2-3}$.

$=u_{2-3}$ and $b_1\neq b_3$) the front has nonzero velocity. But now the front profile may be different from front profile in the bistable model due to the middle interfacial zone. When the size of this zone u_0 is slightly below the critical value $u_{\rm crit}$ the front curve has a knee [Fig. 2(a)]. When u_0 is significantly less than $u_{\rm crit}$, the knee disappears [Fig. 2(b)]. The knee is more pronounced when ξ_0^* is large enough. And when $u_0\to u_{\rm crit}$ the matching point coordinate $\xi_0^*\to\infty$ and the tristable front degenerates into bistable front (between $u=-b_3$ and $u=0$).[2]

Now we consider the 4-front. In this case the solution can be written as

$$u_1(\xi)=A_1e^{\lambda^+\xi}-b_1, \quad \xi\leqslant\xi_0,$$

$$u_2(\xi)=A_{21}e^{\lambda^+\xi}+A_{22}e^{\lambda^-\xi}, \quad \xi_0\leqslant\xi\leqslant\xi_0^*,$$

$$u_3(\xi)=A_{31}e^{\lambda^+\xi}+A_{32}e^{\lambda^-\xi}+b_3, \quad \xi_0^*\leqslant\xi\leqslant\xi_0^{**}, \qquad (7)$$

$$u_4(\xi)=A_4e^{\lambda^-\xi}, \quad \xi\geqslant\xi_0^{**},$$

where $\lambda^\pm$ are the same as above. The matching conditions (4) and (5) are now supplemented with three additive equations at the third matching point $\xi=\xi_0^{**}$: $u_3(\xi_0^{**})=u_4(\xi_0^{**}), du_3(\xi_0^{**})/d\xi=du_4(\xi_0^{**})/d\xi$, and $u_4(\xi_0^{**})=u_{2-3}$. The derivation of the front parameters is the same as in the 3-front case and we omit here the details. This front solution is shown in Fig. 3. The front curve is similar to the front profile for the activator variable in the two-component bistable system: there is a hump in the front profile $u(\xi)$.[3] The velocity of the 4-front has nonzero value for the symmetric null-cline case as opposed to the 3-front case and this

[1]In Ref. [5] was considered a potential with three equal maxima. Therefore, in this case there exist only solutions between two neighbor maxima.

[2]It should be noted here also that the three-piece front with middle interfacial zone may exist in the bistable model which is characterized by the positive slope coefficient of the middle part of three-pieces null-cline function $f(u)=0$ [18].

[3]There are no humps in the bistable one-component model. A hump can appear in the case of nonlocal equations (with an integral convolution in space) [19].

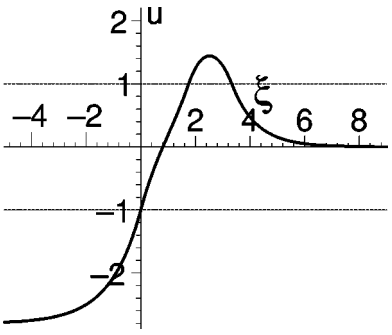

FIG. 3. Front solution (7) in the case of symmetric null-cline.

fact can be again explained using the particle-in-a-potential picture. The speed magnitude is dependent on the null-cline choice. When the size of outer zones becomes larger the front velocity grows also.

III. EXTERNAL PERIODIC FORCING

In this section we estimate the influence of external forcing. To introduce an external forcing $\overline{f}(x,t)$, the model equation is modified as

$$\frac{\partial u(x,t)}{\partial t} = f(u) + \overline{f}(x,t) + \frac{\partial^2 u(x,t)}{\partial x^2}. \tag{8}$$

Passing to the traveling frame coordinate ξ we consider the case when the forcing $\overline{f}$ is *nonmoving* in the comoving frame, i.e., it is a function of only ξ. Then the traveling wave equation reads

$$\frac{d^2u(\xi)}{d\xi^2} + c\frac{du(\xi)}{d\xi} + f(u) + \overline{f}(\xi) = 0. \tag{9}$$

The simplest case of the periodic forcing $\overline{f}(\xi)$ may be presented by the following expression: $\overline{f}(\xi) = \cos(k\xi)$. It is not necessary for us to assume in the following that the oscillations of the forcing are slow and the considered fronts may be described to the needed accuracy within the adiabatic approximation [12]. We will find the wave solution exactly.

Performing the stability analysis of the fronts in the homogeneous equation it can be shown that the 3-front is stable, whereas the 4-front is unstable. Therefore, it is pertinent to consider below only 3-front. The 3-front solution of Eq. (9) takes the form

$$\begin{aligned} u_1(\xi) &= A_1 e^{\lambda^+ \xi} - b_1 + \overline{u}(\xi), \quad \xi \leqslant \xi_0, \\ u_2(\xi) &= A_{21} e^{\lambda^+ \xi} + A_{22} e^{\lambda^- \xi} + \overline{u}(\xi), \quad \xi_0 \leqslant \xi \leqslant \xi_0^*, \\ u_3(\xi) &= A_3 e^{\lambda^- \xi} + b_3 + \overline{u}(\xi), \quad \xi \geqslant \xi_0^*, \end{aligned} \tag{10}$$

where $\overline{u}(\xi) = R\cos(k\xi) + Q\sin(k\xi)$ and $R, Q = \text{const}$. To determine the constants R and Q we insert $\overline{u}(\xi)$ into Eq. (9) and collect the terms multiplied by $\cos(k\xi)$ and $\sin(k\xi)$. The result is

$$R = \frac{k^2+1}{(k^2+1)^2 + c^2k^2}, \quad Q = -\frac{ck}{(k^2+1)^2 + c^2k^2}. \tag{11}$$

Hence the constant R is always positive. The sign of Q depends on the combination of parameters ck, Q vanishes when one of these parameters is equal to zero, i.e., for stationary fronts ($c=0$) or constant forcing ($k=0$).

In the preceding section, we chose one matching point value $\xi = \xi_0$ equal to zero. However now, in the presence of the ξ-dependent forcing, the translation invariance of the model equation is violated and the magnitude of the matching point coordinate ξ_0 cannot be chosen arbitrarily[4] or rather, the front solution depends on this value ξ_0, i.e., we have a family of front solutions with different ξ_0.[5] The form of the velocity equation (6) and the expression (A8) for ξ_0^* remain the same because the ξ_0 dependence appears in A constants. With this in mind we obtain the following velocity equation

$$\begin{aligned} &\lambda^- \ln\left\{ \frac{-b_3\lambda^-}{b_1\lambda^+ - 2\gamma[u_{1-2} + \overline{u}(\xi_0)]} \right\} \\ &\quad = \lambda^+ \ln\left\{ \frac{-b_3\lambda^- - 2\gamma[u_{2-3} - \overline{u}(\xi_0^*)]}{b_1\lambda^+} \right\}, \end{aligned} \tag{12}$$

where the second matching point coordinate ξ_0^* is

$$\xi_0^* = \xi_0 + \frac{1}{\lambda^+} \ln\left\{ \frac{-b_3\lambda^-}{b_1\lambda^+ - 2\gamma[u_{1-2} + \overline{u}(\xi_0)]} \right\}. \tag{13}$$

The ξ_0 dependence is present only in the forcing-generated terms, $\overline{u}(\xi)$. The exponential terms with ξ_0 which arose in the matching equations were eliminated during the reduction procedure.

For the sake of simplicity we will now consider the symmetric model with $b_1 = b_3 = 1$ and $u_{1-2} = u_{2-3} \equiv \eta$. Then from the restriction conditions [see Eqs. (6) and (12) for derivation] $(1 + c/2\gamma)/A_{21} > 0$ and $(1 - c/2\gamma)/(A_{22} - A_3) > 0$ it follows that

$$\lambda^+ - 2\gamma[\eta + \overline{u}(\xi_0)] > 0 \quad \text{and} \quad \lambda^- + 2\gamma[\eta - \overline{u}(\xi_0^*)] < 0. \tag{14}$$

Here were used the relationships $1 + c/2\gamma = -\lambda^-/\gamma$ and $1 - c/2\gamma = \lambda^+/\gamma$. The next restriction

[4] If the value of ξ_0 is chosen arbitrarily, as example, $\xi_0 = 0$, the ξ_0 dependence appears in the forcing term $\overline{f}(\xi) = \cos[k(\xi - \xi_0)]$.

[5] The appearance of the ξ_0 dependence in the solutions is not a particular feature of the piecewise linear approximation. It is well known that the nonlinear bistable equation $u_{\xi\xi} + u - u^3 = 0$ has a front solution $u(\xi) = \pm\tanh[(\xi - \xi_0)/\sqrt{2}]$, where $\xi_0 = \text{const}$ is the center of the wave. Due to translational invariance all solutions with variable ξ_0 are similar. But when this invariance is violated [by inserting $\overline{f}(\xi)$ term in the equation] the solutions become different.

$$\overline{u}(\xi_0) > \frac{\lambda^+ + \lambda^-}{2\gamma} - \eta \;\Leftrightarrow\; c/2 + \gamma\overline{u}(\xi_0) > -\eta\gamma \quad (15)$$

is evident from the fact that the coordinate ξ_0^* of the second matching point must be larger than the coordinate ξ_0 of the first one. It is appropriate at this point to recall that the velocity equation for fronts in the bistable model (one matching point at ξ_0 and two fixed points at $u = \mp 1$) under forcing reads [20]

$$c/2 + \gamma\overline{u}(\xi_0) = 0 \quad (16)$$

which is a limiting case of Eq. (15) at $\xi_0^* = \xi_0$ and $\eta \to 0$. Since η and γ are positive quantities the region in the velocity diagram bounded by restriction condition (15) incorporates the bistable front velocity curve described by Eq. (16). This curve, the velocity-versus-wave-number dependence $c = c(k)$ at fixed ξ_0, may be monotonic or oscillating according to the value of the matching point coordinate ξ_0 [20]. In the bistable model there is no restrictions on the front velocity.

Together with the first restriction in Eq. (14) the inequality (15) yields the validation interval for $\overline{u}(\xi_0)$:

$$\frac{\lambda^+ + \lambda^-}{2\gamma} - \eta < \overline{u}(\xi_0) < \frac{\lambda^+}{2\gamma} - \eta, \quad (17)$$

which in the case of stationary fronts (when $c = 0$) reduces to $-\eta < \overline{u}(\xi_0) < 1/2 - \eta$. The origin of the restriction conditions (14) is of the same kind as one in the system without forcing (see Sec. I). This fact permits us to do away with a more sophisticated treatment of these restrictions and turn our attention to the discussion of the velocity equation (12). From this equation it follows that the front velocity is a function of wave number k and phase (matching point coordinate) ξ_0 when the null-cline parameter η is fixed. The wave number is a control parameter, whereas the front solution is uniquely determined by phase value. All solutions are conveniently grouped together in a velocity-versus-phase diagram. These diagrams are shown in Fig. 4. The velocity dependence (16) for the bistable front is added in the figures for comparison. Both (for tristable and bistable models) velocity-versus-phase curves are typified by oscillating behavior around $c = 0$ axis, so that there exist fronts with positive and negative velocities. However, the velocity curve for the tristable front is irregular in shape near $\xi_0 \approx 0.5$ [Fig. 4(a)]. This irregularity is easily observable when the wave number is small enough. As this takes place, a new solution for the tristable case appears [at $\xi_0 \approx 0.4$ and $c = 0$ in Fig. 4(b)]. This solution corresponds to an isolated point on the $\xi_0 - c$ diagram and presents a stationary front. At this time the oscillating curve for the velocity of the tristable front becomes more irregularly shaped. The point transforms to the bubble as the control parameter decreases [Fig. 4(c)], i.e., a set of nonstationary front solutions occurs also. The bubble is out of round and grows with decreasing wave number. At some values of k the bubble meets the main oscillation line [Fig. 4(d)] and after this breaks it and forms a curve of combined shape [Fig. 4(e)]. The shape of bubble-transformed branch repeats the main curve with further decreasing control parameter [Fig. 4(f)]. However, it should be particularly emphasized that such calculations cannot be carried out with similar success for sufficiently small k, because in this case the front profile oscillation in the middle interfacial zone leaves this zone, i.e., there are more than two matching points. In this paper we consider only two matching point procedures.

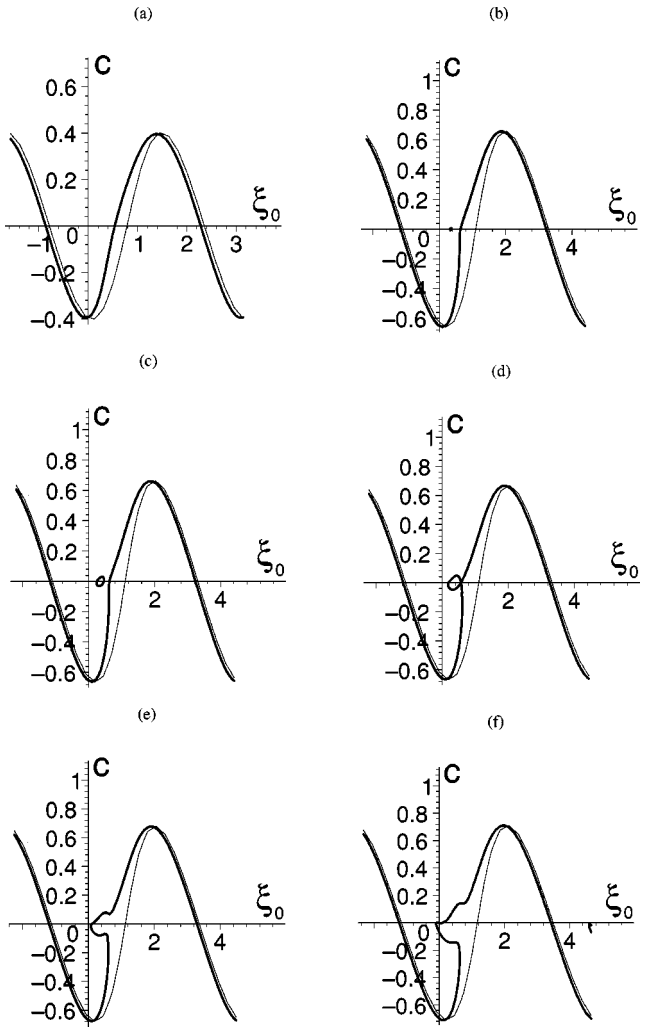

FIG. 4. Velocity-versus-phase dependences. The tristable cases (12) and (13) with symmetric null-cline $b_1 = b_3 = 1$ and $u_{1-2} = u_{2-3} \equiv \eta = 0.1$ are denoted by thick line. The bistable case (16) with the same fixed point coordinates is denoted by thin line. The values of the control parameter are (a) $k = 2$, (b) $k = 1.43$, (c) $k = 1.425$, (d) $k = 1.418$, (e) $k = 1.4$, (f) $k = 1.35$.

The bubble formation and the curve irregularity conversion are a characteristic feature of the tristable system. They are well represented in the case of stationary fronts when $c = 0$. The zeros of the front velocity uniquely characterize the stationary front solutions and in analogy to solid state physics we call these solutions pinned fronts, so that the zeros of the velocity curve indicate pinning positions. When $c = 0$ the velocity equation (12) is reduced to

$$\overline{u}(\xi_0^*) = -\overline{u}(\xi_0), \quad (18)$$

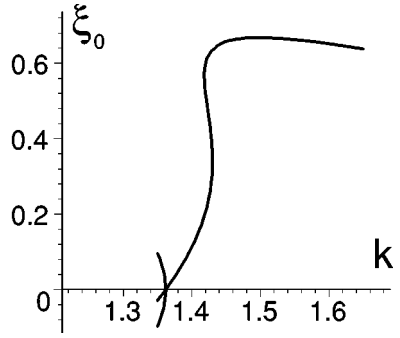

FIG. 5. Bifurcation diagram for the stationary fronts. The values of the null-cline parameters are the same as for Fig. 4. The values of control parameter are sufficiently large, $k \geqslant 1.35$. In this case the front profile oscillations will stop short of reaching the matching point coordinates $-u_{1-2}$ and u_{2-3} [see also a comment after Fig. 4(f) in the paper].

where

$$\xi_0^* = \xi_0 - \ln\{1 - 2[\eta + \overline{u}(\xi_0)]\}. \tag{19}$$

Inserting the expression for the periodic forcing $\overline{u}(\xi)$ into Eqs. (18) and (19) after some manipulations we obtain

$$\frac{\cos(k\xi_0)}{k^2+1} = \frac{1}{2}\{1 - \exp[2\xi_0 - (\pi + 2\pi n)/k]\} - \eta,$$

$$\frac{\cos(k\xi_0)}{k^2+1} = \frac{1}{2}\{1 - \exp[-(\pi + 2\pi n)/k]\} - \eta, \tag{20}$$

$$n = 0, \pm 1, \pm 2, \ldots .$$

These equations describe $k - \xi_0$ dependences which are shown in Fig. 5 in the vicinity of the bifurcation points. In the range under consideration in this figure the curves are presented by $n=0$ case of Eq. (20). We notice that there are two different bifurcations on the interval from $k=1.6$ to $k=1.3$. The first bifurcation near $k \approx 1.43$ corresponds to the bubble formation on the ξ_0-c diagram (in Fig. 4). The key feature of this phenomenon is a multivalued dependence of the phase ξ_0 on the control parameter k on the interval from $k \approx 1.43$ to $k \approx 1.42$ in Fig. 5. The multivalued curve folds to form three connected branches. The branches terminate at some critical values. The termination points indicate a spontaneous front transition between two branches when the front is phase shifted. The second bifurcation at $k \approx 1.36$ is a pitchfork bifurcation and forms two symmetric branches [which are described by the second equation in Eq. (20) at $n=0$] with opposite phases along with one asymmetric branch which changes the sign of the phase at the bifurcation point.

It is anticipated that similar bifurcations exist on the velocity-versus-wave-number diagram at some fixed phases. However, we expect that the phase values for the bifurcation points are different. By these bifurcations forms a pair of counterpropagating fronts which can lead to the formation of complex spatiotemporal patterns in a like manner as for nonequilibrium Ising-Bloch bifurcation of the bistable fronts [21–23]. This effect is of importance because the front bifurcation may show where in parameter space it should expect an initial pattern of domains to decay toward a uniform state and where to develop into a stable traveling wave.

IV. CONCLUSION

Piecewise linear tristable reaction-diffusion equation under periodic forcing was considered. Matching procedures of fronts were performed analytically. Exact analytical solutions were obtained for the propagating front and the front velocity. Two basic types of the tristable fronts, monotone and nonmonotone (the 3- and 4-fronts), were considered. The influence of external periodic forcing was estimated. The simple form of the periodic force $\cos(k\xi)$ was used. The analysis of forced reaction-diffusion equation predicts sets of possible solutions (fronts with positive, negative, and zero velocities). These solutions are distinguished by their phases (matching point coordinates ξ_0). The velocity-versus-phase diagram shows the formation of the additional solution set (bubble formation) for the specific choice of wave number along with basic oscillating curve. This phenomenon corresponds to the bifurcation on the phase-versus-wave-number diagram (at fixed velocity). The observed bifurcation is the characteristic feature of the tristable model under periodic forcing and we have every reason to believe that this effect is of importance because it can lead to the formation of complex spatiotemporal patterns just as in the bistable systems.[6] The main effect of the front bifurcation, regarding spatiotemporal patterns, is the formation of stable traveling domain patterns. The change in the qualitative behavior of patterns can be attributed to the appearance of the front multiplicity at the bifurcation [23]. This implies that along with a front that transforms the lower state to the upper state, there exists another front propagating in the same direction that transforms the upper state back to the lower one. A combination of the two, using appropriate initial conditions, can yield diverse traveling domain structures (two fronts following one another) [23]. We have not explored here the implication of the observed phenomena on pattern formation because we confined ourselves in this paper to solitary traveling fronts.

The external forcing consideration works very well. In Ref. [24] another type of forcing, presented as spatial inhomogeneities $\overline{f}(x)$, was analyzed to describe a bifurcation of front dynamics. The case of pure temporal forcing $\overline{f}(t)$ was considered in Refs. [12,25]. However, when traveling wave solutions are examined, it makes no significant difference whether temporal $\overline{f}(t)$ or spatial $\overline{f}(x)$ external forcing is employed, because in both cases we have the same null-cline with time- or space-dependent parameters which indicate zeros of the rate function $f(u)$. Therefore, the ''traveling forcing'' $\overline{f}(\xi)$ considered in our paper becomes a subject of much specific interest.

[6] A front bifurcation in the periodically forced complex Ginzburg-Landau equation which describes spatiotemporal modulations of an oscillating medium has been found by Coullet *et al.* [21].

The studies of the tristable model lead to the generalization of results known earlier in the bistable systems. Moreover, the solution (3) may describe a pulse wave in a two-piece system when the third piece of null-cline is coincident with the first piece, i.e., when $u_{2-3}=-u_{1-2}$ and $b_3=-b_1$ and the pulse interpolates from $u=-b_1$ as $\xi\to-\infty$ to $u=-b_1$ as $\xi\to+\infty$. Naturally, the restriction condition transforms into only one equation ($u_{1-2}>b_1/2$ for the motionless wave). Thus, in the case of the pulse wave in the two-piece system the null-cline must be always asymmetric. This fact is well known in the bistable model with piecewise linear and cubic polynomial $f(u)=u(1-u)(u-a)$ functions [14]: for $a>1/2$ the nerve goes dead, i.e., the only trivial traveling wave solution is $u\equiv 0$. Therefore, we suppose that above-mentioned restriction for the middle interfacial zone in the tristable model has the same origin as we have for the pulse in the bistable system. We assume also that this restriction holds for the tristable model with continuous (quintic) reaction term $f(u)$.

The approach employed in investigation of the reaction-diffusion equation of parabolic type bears close similarity to those used in the study of fronts in the equation of hyperbolic type [16]. Conventional techniques are a great convenience in this case. It is not improbable that in the tristable hyperbolic reaction-diffusion equation exist fronts with spatial oscillations as it was found in the case of front propagation into a metastable state [16]. The question only arises of whether there are significant differences in front propagation in the parabolic and hyperbolic models.

Further investigation of the tristable reaction-diffusion system is required towards the modeling of the front dynamics in a two-component system. The two-component bistable systems have been much studied [15,22,23]. The velocity diagrams show a pitchfork bifurcation [22,23] and front solutions differ not only in their propagation direction but also in their internal structure. A complete analytical stability analysis of fronts has also been performed [17]. Thus, we now have the machinery at our disposal to generalize to the two-component case without the need of entering into numerics immediately.

ACKNOWLEDGMENTS

The author thanks A. L. Kawczyński for introduction to the problem and V. S. Zykov and A. S. Mikhailov for useful comments. This work was supported by the *Deutsche Forschungsgemeinschaft* under Grant No. FOR 301/2-1 (3) in the framework of a research group on ''Interface dynamics in pattern forming processes.''

APPENDIX

1. 3-front

First of all, we calculate the front parameters. Inserting the solution (3) into matching conditions (4), we write the equations

$$A_1-b_1=A_{21}+A_{22}, \tag{A1}$$

$$A_1\lambda^+=A_{21}\lambda^++A_{22}\lambda^-, \tag{A2}$$

$$A_1-b_1=-u_{1-2}, \tag{A3}$$

$$A_{21}e^{\lambda^+\xi_0^*}+A_{22}e^{\lambda^-\xi_0^*}=A_3e^{\lambda^-\xi_0^*}+b_3, \tag{A4}$$

$$A_{21}\lambda^+e^{\lambda^+\xi_0^*}+A_{22}\lambda^-e^{\lambda^-\xi_0^*}=A_3\lambda^-e^{\lambda^-\xi_0^*}, \tag{A5}$$

$$A_3e^{\lambda^-\xi_0^*}+b_3=u_{2-3}. \tag{A6}$$

First we consider Eqs. (A4) and (A5). Multiplying Eq. (A4) by $c/2$ and inserting the result into Eq. (A5), where $\lambda^\pm=-c/2\pm\gamma$ was used, we obtain a pair of equations

$$A_{21}e^{\lambda^+\xi_0^*}+(A_{22}-A_3)e^{\lambda^-\xi_0^*}=b_3, \tag{A4$'$}$$

$$\gamma[A_{21}e^{\lambda^+\xi_0^*}-(A_{22}-A_3)e^{\lambda^-\xi_0^*}]=\frac{c}{2}b_3. \tag{A7}$$

By addition and subtraction of Eqs. (A4) and (A7) we can eliminate

$$\xi_0^*=\frac{1}{\lambda^+}\ln\left[\frac{b_3\left(1+\frac{c}{2\gamma}\right)}{2A_{21}}\right]=\frac{1}{\lambda^-}\ln\left[\frac{b_3\left(1-\frac{c}{2\gamma}\right)}{2(A_{22}-A_3)}\right] \tag{A8}$$

and derive the velocity Eq. (6).

Now we determine the constants A. $A_1=b_1-u_{1-2}$ and A_{21},A_{22} we find from Eqs. (A1) and (A2). The procedure is the same as above. We multiply Eq. (A1) by $c/2$ and insert the result into Eq. (A2), where $\lambda^\pm=-c/2\pm\gamma$ was used. The result reads

$$(A_{21}-A_1)+A_{22}=-b_1, \tag{A1$'$}$$

$$\gamma[(A_{21}-A_1)-A_{22}]=-\frac{c}{2}b_1, \tag{A9}$$

and by addition and subtraction of Eqs. (A1) and (A9) we obtain the constants

$$A_{21}=\frac{b_1}{2}\left(1-\frac{c}{2\gamma}\right)-u_{1-2}, \tag{A10}$$

$$A_{22}=-\frac{b_1}{2}\left(1-\frac{c}{2\gamma}\right). \tag{A11}$$

From Eq. (A6) we derive A_3 using expressions for A_{22} and $e^{\lambda^-\xi_0^*}$,

$$A_3=-b_1\frac{(u_{2-3}-b_3)\left(1-\frac{c}{2\gamma}\right)}{b_3\left(1-\frac{c}{2\gamma}\right)+2(u_{2-3}-b_3)}. \tag{A12}$$

2. Under forcing

From the matching equations it follows that

$$A_1 e^{\lambda^+ \xi_0} - b_1 = A_{21} e^{\lambda^+ \xi_0} + A_{22} e^{\lambda^- \xi_0}, \tag{A13}$$

$$A_1 \lambda^+ e^{\lambda^+ \xi_0} = A_{21} \lambda^+ e^{\lambda^+ \xi_0} + A_{22} \lambda^- e^{\lambda^- \xi_0}, \tag{A14}$$

$$A_1 e^{\lambda^+ \xi_0} - b_1 + \overline{u}(\xi_0) = -u_{1-2}, \tag{A15}$$

$$A_{21} e^{\lambda^+ \xi_0^*} + A_{22} e^{\lambda^- \xi_0^*} = A_3 e^{\lambda^- \xi_0^*} + b_3, \quad \text{[Eq. (A4)]}$$

$$A_{21} \lambda^+ e^{\lambda^+ \xi_0^*} + A_{22} \lambda^- e^{\lambda^- \xi_0^*} = A_3 \lambda^- e^{\lambda^- \xi_0^*}, \quad \text{[Eq. (A5)]}$$

$$A_3 e^{\lambda^- \xi_0^*} + b_3 + \overline{u}(\xi_0^*) = u_{2-3}. \tag{A16}$$

On rearrangement, the results can be written as

$$A_1 = [b_1 - u_{1-2} - \overline{u}(\xi_0)] e^{-\lambda^+ \xi_0}, \tag{A17}$$

$$A_{21} = \left[\frac{b_1}{2} \frac{\lambda^+}{\gamma} - u_{1-2} - \overline{u}(\xi_0) \right] e^{-\lambda^+ \xi_0}, \tag{A18}$$

$$A_{22} = -\frac{b_1}{2} \frac{\lambda^+}{\gamma} e^{-\lambda^- \xi_0}, \tag{A19}$$

$$A_3 = \frac{u_{2-3} - b_3 - \overline{u}(\xi_0^*)}{\dfrac{b_3 \lambda^+}{2\gamma} + u_{2-3} - b_3 - \overline{u}(\xi_0^*)} A_{22}. \tag{A20}$$

[1] J. D. Murray, *Mathematical Biology* (Springer, Berlin, 2002).
[2] A. S. Mikhailov, *Foundations of Synergetics I. Distributed Active Systems* (Springer, Berlin, 1994).
[3] M.C. Cross and P.C. Hohenberg, Rev. Mod. Phys. **65**, 851 (1993).
[4] M. Leda and A. L. Kawczyński, in *Proceedings of the Third European Interdisciplinary School on Nonlinear Dynamics EUROATTRACTOR 2003*, edited by W. Klonowski (unpublished).
[5] K. Rajchel, Acta Phys. Pol. A **79**, 417 (1991).
[6] E.M. Maslov and A.G. Shagalov, Physica D **152–153**, 769 (2001).
[7] K.I. Agladze, V.A. Davydov and A.S. Mikhailov, Pis'ma Zh. Eksp. Teor. Fiz. **45**, 601 (1987) [JETP Lett. **45**, 767 (1987)].
[8] O. Steinbock, V.S. Zykov, and S.C. Müller, Nature (London) **366**, 322 (1993).
[9] M. Braune and H. Engel, Chem. Phys. Lett. **211**, 534 (1993).
[10] V.N. Biktashev and A.V. Holden, J. Theor. Biol. **169**, 101 (1994).
[11] S. Grill, V.S. Zykov, and S.C. Müller, Phys. Rev. Lett. **75**, 3368 (1995).
[12] F.G. Bass and R. Bakanas, Europhys. Lett. **53**, 444 (2001).
[13] V. S. Zykov, *Simulation of Wave Processes in Excitable Media* (Manchester University Press, New York, 1987).
[14] H.P. McKean, Adv. Math. **4**, 209 (1970).
[15] A. Ito and T. Ohta, Phys. Rev. A **45**, 8374 (1992).
[16] K.K. Manne, A.J. Hurd, and V.M. Kenkre, Phys. Rev. E **61**, 4177 (2000).
[17] E.P. Zemskov, V.S. Zykov, K. Kassner, and S.C. Müller, Nonlinearity **13**, 2063 (2000).
[18] R. Bakanas, Nonlinearity **16**, 313 (2003).
[19] S.A. Gourley, J. Math. Biol. **41**, 272 (2000).
[20] E.P. Zemskov, K. Kassner, and S.C. Müller, Eur. Phys. J. B **34**, 285 (2003).
[21] P. Coullet, J. Lega, B. Houchmanzadeh, and J. Lajzerowicz, Phys. Rev. Lett. **65**, 1352 (1990).
[22] A. Hagberg and E. Meron, Chaos **4**, 477 (1994).
[23] A. Hagberg and E. Meron, Nonlinearity **7**, 805 (1994).
[24] P. Schütz, M. Bode, and H.-G. Purwins, Physica D **82**, 382 (1995).
[25] V.S. Zykov, A.S. Mikhailov, and S.C. Müller, Phys. Rev. Lett. **78**, 3398 (1997).